A Study of Structure and Dynamic Stereochemistry in Seven Coordination: $HMo[P(OCH_3)_3]_4[O_2CCF_3]$[1]

S. S. Wreford,[*2a] **J. K. Kouba, J. F. Kirner, E. L. Muetterties,**[*2b]
I. Tavanaiepour, and V. W. Day[*2c,d]

Contribution from the Department of Chemistry, Harvard University, Cambridge, Massachusetts 02138, the Department of Chemistry, University of California, Berkeley, California 94720, and the Department of Chemistry, University of Nebraska, Lincoln, Nebraska 68588. *Received August 13, 1979*

Abstract: The crystal and molecular structure of $HMo[P(OCH_3)_3]_4[O_2CCF_3]$ was solved by a three-dimensional X-ray crystallographic study. This seven-coordinate complex crystallized in monoclinic form in the centrosymmetric space group $P2_1/n$ with lattice constants of a = 15.456 (2) Å, b = 12.415 (2) Å, c = 15.589 (2) Å, and β = 95.03 (1)° and with four molecules per unit cell. For the idealized description of molecular geometry, the pentagonal bipyramidal form is appropriate, although there is a departure from this form toward an alternative idealized form, the capped octahedron. In terms of an idealized pentagonal bipyramid, two of the phosphite ligands occupy axial coordination sites and the other two are separated by the hydride ligand in the equatorial girdle. Salient coordination sphere structural parameters are Mo–H = 1.59 (4) Å, $Mo–P_{EQ}$ = 2.322 (av) Å, $Mo–P_{AX}$ = 2.404 (av) Å, and Mo–O = 2.317 (av) Å. Within the context of the idealized pentagonal bipyramidal geometry, there is a distortion from idealized L–M–L angles that is counter to ligand–ligand nonbonded interactions and is suggestive of an electronic effect. Expectedly, this seven-coordinate molecule was stereochemically nonrigid. NMR line shape analysis established the permutational character of the intramolecular exchange process. The dominant permutational character of the exchange process is not that associated with the expected facile interconversion of pentagonal bipyramidal, capped octahedral, and capped trigonal prismatic polyhedral forms—provided that there is no intermediate of finite concentration (nonmutual exchange). The exchange process is in effect a nonpairwise exchange between inequivalent phosphorus atom environments. Either there is an exchange intermediate of substantial concentration or else a dominant exchange process that does not follow any of the simple idealized geometric paths that interconnect the aforementioned idealized geometries.

Introduction

Seven coordination is possibly the most complicated subject in the structural and dynamic stereochemical aspects of coordination chemistry.[3,4] These aspects are of considerable importance to an understanding of associative and dissociative reactions of six- and eight-coordinate complexes, respectively.[4] Only a more extensive set of structural and stereochemical data can yield a thorough understanding of seven coordination because the structural and stereochemical issues here possess a subtlety that cannot be resolved fully by theoretical analysis.[4] We describe here the crystal and molecular structure and the dynamic stereochemistry of an unusual seven-coordinate molybdenum hydride, $HMo[P(OCH_3)_3]_4[O_2CCF_3]$.

Experimental Section

Crystallographic Studies. Large, black-red single crystals of $HMo[P(OCH_3)_3]_4[O_2CCF_3]$, suitable for X-ray studies, were grown from pentane.[1] Preliminary photographic studies using Weissenberg and precession techniques indicated monoclinic, $2/m$, symmetry. The systematically absent reflections were those uniquely required by the centrosymmetric space group $P2_1/n$ [an alternate setting of $P2_1/c$-C_{2h}^5 (no. 14)[5]]. This choice was fully supported by all stages of the subsequent structure determination and refinement.

An irregularly shaped crystal with maximum and minimum dimensions of 0.80 and 0.65 mm, respectively, was glued to the inside of a thin-walled glass capillary under nitrogen for all subsequent X-ray studies. This crystal was then accurately centered optically on a computer-controlled four-circle Syntex P$\bar{1}$ autodiffractometer and a total of 15 high-angle ($2\theta_{MoK\bar{\alpha}} > 40°$) reflections, chosen to give a good sampling of reciprocal space and diffractometer settings, were used to align the crystal and calculate angular settings for each reflection. A least-squares refinement of the diffraction geometry for these 15 reflections recorded at the ambient laboratory temperature of 20 ± 1 °C with graphite-monochromated Mo K$\bar{\alpha}$ radiation (λ = 0.710 73 Å) gave the lattice constants a = 15.456 (2) Å, b = 12.415 (2) Å, c = 15.589 (2) Å, and β = 95.03 (1)°. A unit cell content of four $HMo[P(OCH_3)_3]_4[O_2CCF_3]$ molecules per 2980 Å^3 gave a calculated density of 1.56 g/cm^3. The linear absorption coefficient of the crystal for Mo K$\bar{\alpha}$ radiation[6] is 0.71 mm^{-1}.

Intensity measurements utilized graphite-monochromated Mo K$\bar{\alpha}$ radiation and the ω scanning technique with a 4° take-off angle and a normal-focus X-ray tube. For those reflections having $2\theta_{MoK\bar{\alpha}} < 43°$, a scanning rate of 3°/min was employed for the scan between ω settings 0.50° above and below the calculated K$\bar{\alpha}$ doublet value of each reflection. A scanning rate of 2°/min was used for reflections having $43° < 2\theta < 55°$ and a scanning rate of 1°/min was used for the remaining reflections. Each 1° scan was divided into 19 equal time intervals and those 13 contiguous intervals which had the highest single accumulated count at their midpoint were used to calculate the net intensity from scanning. A careful and systematic preliminary study of peak widths (half-height to half-height) indicated a nearly constant peak width of 0.28° in ω for all orientations of the crystal. Background counts, each lasting for one-half the total time used for the net scan, were measured at ω settings 1° above and below the calculated value for each reflection.

A total of 10 220 independent reflections having $2\theta_{MoK\bar{\alpha}} < 63.7°$ (the equivalent of 1.5 limiting Cu K$\bar{\alpha}$ spheres) were measured in concentric shells of increasing 2θ containing approximately 3400 reflections each. The six standard reflections, measured every 300 reflections as a monitor for possible disalignment and/or deterioration of the crystal, gave no indication of either. The intensities were reduced without absorption corrections to relative squared amplitudes, $|F_o|^2$, by means of standard Lorentz and polarization corrections.

Of the 10 220 reflections examined, 3346 were eventually rejected as unobserved by applying the rejection criterion, $I < 3.0\sigma(I)$, where $\sigma(I)$ is the standard deviation in the intensity computed from

$$\sigma^2(I) = (C_t + K^2B)$$

C_t being the count from scanning, K the ratio of scanning time to background time (in this case, K = 1), and B the total background count. The heavy-atom technique, difference Fourier syntheses, and full-matrix least-squares refinement were used with the remaining 6874 observed intensities in the determination and refinement of the structure.

After the atomic coordinates of the molybdenum atom were derived from a three-dimensional Patterson synthesis, the remaining nonhydrogen atoms of the totally general-position asymmetric unit were located from a series of least-squares refinement cycles followed by difference Fourier syntheses. Unit-weighted full-matrix least-squares refinement of the fractional atomic coordinates and isotropic thermal parameters of the 36 crystallographically independent nonhydrogen

0002-7863/80/1502-1558$01.00/0

atoms resulted in a conventional unweighted residual

$$R_1 = \sum||F_o| - |F_c||/\sum|F_o|$$

of 0.096 and a conventional weighted residual

$$R_2 = \{\sum w(|F_o| - |F_c|)^2/\sum w|F_o|^2\}^{1/2}$$

of 0.098 for 2977 independent reflections having $2\theta_{\mathrm{Mo}K\bar{\alpha}} < 43°$ and $I > 3\sigma(I)$. These and all subsequent structure factor calculations employed the atomic form factors compiled by Cromer and Mann[7] and an anomalous dispersion correction to the scattering factor of the molybdenum and four phosphorus atoms.[8] Utilization of anisotropic thermal parameters for all nonhydrogen atoms in further cycles of least-squares refinement gave $R_1 = 0.045$ and $R_2 = 0.054$ for 2977 reflections.

A difference Fourier synthesis based on this fully refined anisotropic model contained peaks which corresponded to chemically anticipated positions of the 37 hydrogen atoms. The most intense peak was that of the hydride ligand. Further unit-weighted least-squares minimization of the function $\sum w(|F_o| - k^{-1}|F_c|)^2$ (where w is the weight assigned to each reflection and k is the scale factor which puts F_o on an absolute basis), which employed isotropic thermal parameters for hydrogen atoms but was otherwise anisotropic, gave $R_1 = 0.031$ and $R_2 = 0.030$ for 2977 reflections. All subsequent refinement cycles employed a least-squares refineable extinction correction[9] of the form $1/(1 + gI_c)$ where the extinction coefficient, g, refined to a final value of 1.57×10^{-7}. Additional cycles of unit-weighted full-matrix least-squares refinement with those reflections having $2\theta_{\mathrm{Mo}K\bar{\alpha}} < 63.7°$ resulted in $R_1 = 0.033$ and $R_2 = 0.032$ for 6874 reflections having $I > 3\sigma(I)$.

Empirical weights ($w = 1/\sigma^2$) were then calculated from

$$\sigma = \sum_{0}^{2} a_n F_o{}^n = 0.605 + 0.873 \times 10^{-2}F_o - 0.821 \times 10^{-5}F_o{}^2$$

the a_n being coefficients derived from the least-squares fitting of the curve

$$||F_o| - |F_c|| = \sum_{0}^{2} a_n|F_o|^n$$

where the F_c values were calculated from the fully refined model using unit weighting and an $I > 3\sigma(I)$ rejection criterion. The final cycles of empirically weighted least-squares refinement which employed isotropic thermal parameters for hydrogen atoms and anisotropic thermal parameters for all others converged to final values of 0.033 and 0.042 for R_1 and R_2, respectively, for 6874 independent reflections.[10] During the final cycles of refinement, no parameter (including those of the hydrogen atoms) shifted by more than $0.65\sigma_p$ with the average shift being less than $0.05\sigma_p$ where σ_p is the estimated standard deviation of the parameter.

The following programs were used on an IBM 360/65 or 370/148 computer for this work: MAGTAP, SCALUP, and SCTFT2, data reduction programs written by V. W. Day; FORDAP, Fourier and Patterson synthesis program, a modified version of A. Zalkin's program; ORFLSE, full-matrix least-squares structure refinement program, a highly modified version of Busing, Martin, and Levy's original ORFLS; ORFFE, bond lengths and angles with standard deviations by Busing, Martin, and Levy; ORTEP2, thermal ellipsoid plotting program by Johnson; MPLANE, least-squares mean-plane calculation program from L. Dahl's laboratory.

NMR Studies. NMR spectra were recorded on Bruker HX-90 and Varian XL-100 spectrometers. Line-shape calculations were performed on IBM 360/91 and PDP-11 computers using Binsch and Kleier's DNMR-3[11] program as modified by Bushweller.[12] In addition, the program was modified to allow variation of the exchange-independent line width after calculation of the spectral eigenvectors. For each transition, the real part of the contracted spectral vector, D, is a function of the value input for T_2, REAL(D) = $X - 1/T_2$, where X represents exchange broadening. Thus by modifying the value of REAL(D), the value of the exchange-independent line width was varied.

Results and Discussion

Solid-State Structure of $HMo[P(OCH_3)_3]_4[O_2CCF_3]$. Final atomic coordinates for all atoms and anisotropic thermal parameters for the nonhydrogen atoms are given in Tables I and II,[10] respectively. The numbering scheme used to designate atoms of the $HMo[P(OCH_3)_3]_4[O_2CCF_3]$ molecule (**1**) is as follows. Atoms of the four phosphite ligands are distinguished from each other by a (first) numerical subscript to the appropriate atomic symbol. Phosphite oxygen and carbon atoms carry a second numerical subscript to distinguish between different methoxy arms of the same ligand. Methyl hydrogen atoms contain a third numerical subscript to distinguish between hydrogens on the same carbon. The symbol for the hydride ligand is nonsubscripted and those for atoms of the trifluoroacetate ligand carry a single numerical subscript. A perspective drawing which illustrates this numbering scheme and represents the contents of the asymmetric unit specified by the atomic coordinates of Table I is shown in Figure 1. Bond lengths, polyhedral edge lengths, and bond angles subtended at molybdenum in the coordination group of **1** are given with their estimated standard deviations in Table III. Covalent bond lengths and angles for nonhydrogen atoms of the trimethyl phosphite and perfluoroacetate ligands are given with estimated standard deviations in Table IV; phosphite bond lengths and angles involving hydrogen atoms are given in Table V.[10]

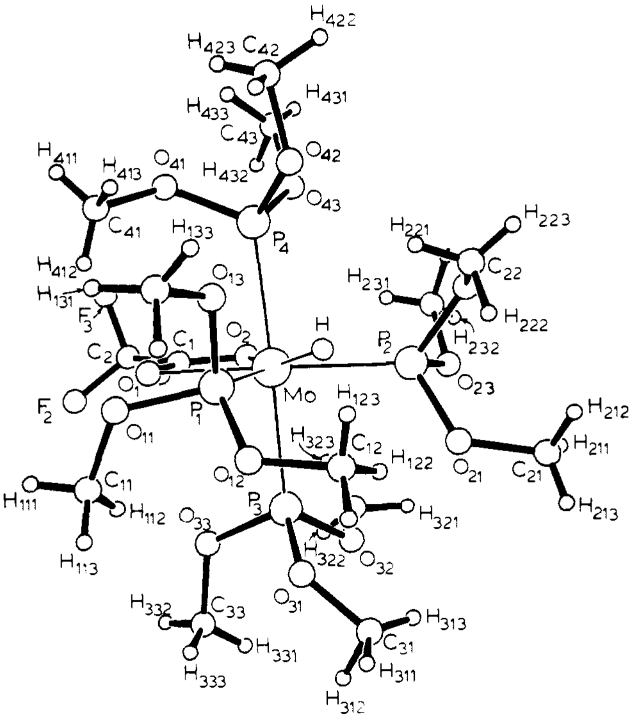

Figure 1. Perspective drawing (adapted from an ORTEP plot) of the solid-state structure of $HMo[P(OCH_3)_3]_4(O_2CCF_3)$ (**1**). For purposes of clarity, all atoms are represented by arbitrarily sized open circles which are in no way representative of their true thermal motion. The coordination group approximates C_s-m symmetry with Mo, P_3, P_4, H, and trifluoroacetate carbon atoms C_1 and C_2 ideally lying in the pseudo-mirror plane. The labeling scheme is described in the text; atoms C_{13}, C_{23}, C_{32}, H_{121}, H_{132}, H_{233}, and H_{421} are not labeled in this drawing.

As originally proposed[1] from the NMR analysis of $HMo[P(OCH_3)_3]_4[O_2CCF_3]$, the solid-state coordination geometry closely approximates that of a pentagonal bipyramid with the hydrido ligand, phosphite phosphorus atoms P_1 and P_2, and the two trifluoroacetate oxygen atoms comprising the "pentagonal" girdle and phosphorus atoms P_3 and P_4 occupying the two trans axial coordination sites. This geometry would ideally possess C_{2v} symmetry with H, Mo, and the two acetate carbon atoms lying on the twofold axis, but the actual coordination polyhedron of **1** does not have C_{2v} symmetry and is displaced, as earlier suggested,[1] toward a C_s-m monocapped octahedron (the "nonequatorial" mirror plane is retained). Although Mo, O_1, O_2, P_1, and P_2 are coplanar to within 0.03 Å and their

Table I. Atomic Coordinates in Crystalline $HMo[P(OCH_3)_3]_4(O_2C_2F_3)$[a]

atom type[b]	fractional coordinates			isotropic thermal parameter[c]	atom type[b]	fractional coordinates			isotropic thermal parameter[c]
	10^4x	10^4y	10^4z	B, Å^2		10^3x	10^3y	10^3z	B, Å^2
Mo	−113.5(1)	2500.4(2)	2570.4(1)	2.84	H	37(2)	220(3)	175(2)	3(1)
P_1	−702.2(4)	2747.2(6)	1163.3(4)	3.46	H_{111}	−263(4)	412(5)	130(4)	8(2)
P_2	1389.2(4)	2322.5(5)	2654.3(4)	3.14	H_{112}	−165(3)	442(4)	176(3)	6(1)
P_3	140.0(4)	4386.4(6)	2762.3(5)	3.64	H_{113}	−192(4)	476(5)	94(4)	9(2)
P_4	−404.5(5)	586.5(6)	2586.7(6)	4.09	H_{121}	60(3)	410(4)	−18(3)	5(1)
F_1	−1398(2)	2771(3)	5290(2)	9.9	H_{122}	94(3)	363(4)	83(3)	6(1)
F_2	−2354(3)	3230(5)	4436(3)	11.1	H_{123}	54(3)	292(4)	8(3)	5(1)
F_3	−2081(4)	1652(4)	4627(4)	11.9	H_{131}	−194(4)	164(4)	−7(3)	7(1)
O_{11}	−1705(1)	3117(2)	1045(1)	4.9	H_{132}	−127(5)	229(6)	−63(5)	12(2)
O_{12}	−350(1)	3571(2)	486(1)	4.8	H_{133}	−102(4)	113(5)	−39(4)	10(2)
O_{13}	−809(2)	1663(2)	613(1)	4.8	H_{211}	305(3)	329(4)	281(3)	5(1)
O_{21}	1890(1)	3288(2)	2231(1)	3.8	H_{212}	301(3)	280(3)	196(3)	4(1)
O_{22}	1872(1)	1281(2)	2303(1)	4.1	H_{213}	300(3)	397(4)	204(3)	6(1)
O_{23}	1901(1)	2321(2)	3598(1)	4.4	H_{221}	120(3)	84(3)	123(2)	4(1)
O_{31}	320(2)	5115(2)	1958(2)	5.1	H_{222}	195(3)	163(3)	109(3)	4(1)
O_{32}	935(1)	4825(2)	3417(1)	4.6	H_{223}	216(3)	51(4)	132(3)	6(1)
O_{33}	−678(1)	4988(2)	3137(2)	4.9	H_{231}	122(4)	144(5)	426(4)	10(2)
O_{41}	−1383(1)	183(2)	2649(2)	5.3	H_{232}	207(3)	166(4)	471(3)	6(1)
O_{42}	−85(2)	−154(2)	1840(2)	6.0	H_{233}	186(4)	80(5)	403(3)	8(2)
O_{43}	20(2)	8(2)	3438(2)	6.4	H_{311}	99(4)	605(5)	133(4)	9(2)
O_1	−1458(1)	2701(2)	3070(1)	4.3	H_{312}	80(6)	643(7)	202(6)	16(3)
O_2	−359(1)	2408(2)	4027(1)	4.6	H_{313}	153(4)	562(4)	220(4)	7(1)
C_{11}	−1948(3)	4152(5)	1311(4)	6.7	H_{321}	164(4)	444(4)	454(3)	8(1)
C_{12}	529(3)	3557(4)	264(3)	5.8	H_{322}	70(4)	492(5)	462(4)	8(2)
C_{13}	−1335(4)	1620(5)	−201(3)	6.6	H_{323}	66(3)	385(4)	440(3)	6(1)
C_{21}	2821(2)	3358(3)	2279(3)	4.9	H_{331}	−17(4)	642(5)	354(4)	8(2)
C_{22}	1785(3)	1005(3)	1414(3)	5.3	H_{332}	−109(5)	620(5)	367(4)	11(2)
C_{23}	1744(3)	1503(4)	4200(3)	6.0	H_{333}	−79(2)	639(3)	269(3)	3(1)
C_{31}	1048(3)	5755(4)	1830(4)	6.9	H_{411}	−251(3)	13(3)	206(3)	5(1)
C_{32}	1005(3)	4485(4)	4292(3)	5.7	H_{412}	−217(4)	129(5)	200(4)	10(2)
C_{33}	−669(3)	6125(4)	3309(4)	6.8	H_{413}	−191(5)	34(6)	148(5)	12(2)
C_{41}	−2079(3)	563(4)	2067(4)	6.5	H_{421}	−50(8)	−90(9)	101(7)	21(4)
C_{42}	−378(6)	−1187(6)	1625(8)	11.1	H_{422}	13(6)	−166(7)	164(6)	15(3)
C_{43}	−239(7)	−860(8)	3846(8)	11.8	H_{423}	−88(3)	−130(4)	174(3)	7(1)
C_1	−1146(2)	2557(3)	3822(2)	4.3	H_{431}	1(4)	−115(5)	420(4)	8(2)
C_2	−1759(3)	2537(4)	4532(3)	6.3	H_{432}	−34(6)	−34(7)	423(5)	14(3)
					H_{433}	−77(5)	−117(7)	332(5)	14(3)

[a] Figures in parentheses are the estimated standard deviations for the last significant digit. [b] Atoms are labeled in agreement with Figure 1. [c] For nonhydrogen atoms, this is the equivalent isotropic thermal parameter calculated from $B = 4(V^2 \det(\beta_{ij}))^{1/3}$ where the β_{ij} are the dimensionless anisotropic temperature factors employed during refinement; for hydrogen atoms, this is the isotropic thermal parameter actually refined.

least-squares mean plane[13] makes a dihedral angle of 88.5° with the plane determined by Mo, P_3, P_4, H, C_1, and C_2,[14] the hydride ligand is displaced by 0.41 Å from the "equatorial" five-atom MoO_2P_2 mean plane toward P_4. In the solution state, any displacement of the nominally equatorial hydride ligand (pentagonal bipyramidal form) toward axial phosphite ligands would be of high frequency and would average to zero displacement (see NMR discussion below). The coordination polyhedron of **1** therefore clearly lies along a geometric reaction path that connects the pentagonal bipyramidal and capped octahedral forms. In terms of the monocapped octahedral description, the hydride ligand caps the $P_1\cdots P_2\cdots P_4$ face of an O_2P_4 octahedron and the "lower" triangle determined by O_1, O_2, and P_3 is within 8.7° of being parallel to that determined by P_1, P_2, and P_4. The Mo atom is situated between these two mean planes, being displaced by 1.57 Å from the O_1, O_2, P_3 polyhedral face and by 1.07 Å from the "capped" $P_1\cdots P_2\cdots P_4$ face; the hydride ligand is displaced by 0.43 Å on the opposite side of the "capped" face.

The coordination geometry of **1**, which lies along a path connecting the idealized C_{2v} pentagonal bipyramidal and C_s monocapped octahedral forms, is closer[15] to a pentagonal bipyramid as shown by the data in Table III. The P···P and P···H contacts for the "capped" face are quite dissimilar and would require a ~0.65-Å displacement of the hydride ligand toward P_4 in the pseudo-mirror plane as well as a ~0.35-Å shrinkage of the $P_1\cdots P_2$ polyhedral edge to produce the sets of equivalent P···P and P···H contacts required in a good capped octahedron. A precise placement of the actual coordination polyhedron relative to the idealized polyhedra can be made by an analysis of the dihedral angles generated by normals to the coordination polyhedron only if all ligand atoms are unidentate (or at least chelates with no unusual constraints) and are similar in size and electronic character[15,16]—a condition not satisfied in $HMo[P(OCH_3)_3]_4[O_2CCF_3]$. The observed stereoisomeric arrangement minimizes ligand–ligand repulsions on the coordination sphere for either of these idealized polyhedral descriptions. The small hydride ligand and the small bite of the trifluoroacetate ligand make these ligands well suited for coordination at sites in the congested equatorial girdle of a pentagonal bipyramid or at the face-capping (hydride) site and two of those in the lower triangle (acetate) of a monocapped octahedron. Electronic considerations[4] also would place these ligands in equatorial sites of a pentagonal bipyramid.

The coordination sphere of **1** is quite congested even though three of the sites are occupied by relatively compact ligands. Only the $P_1\cdots P_2$, $P_3\cdots O_1$, $P_2\cdots O_2$, and $P_3\cdots H$ ligand–ligand contacts are greater than the sum of the appropriate van der Waals radii.[17] While the shortest P···O contact is only 0.12 Å less than the van der Waals value of 3.30 Å, all but one of the

Table III. Bond Distances, Polyhedral Edge Lengths, and Angles Subtended at the Mo(II) Atom in the Coordination Polyhedron of $HMo[P(OCH_3)_3]_4(O_2C_2F_3)$[a]

parameter[b]	value	parameter[b]	value
	Distances (Å)		
$Mo-P_1$	2.320(1)	$P_3\cdots O_1$	3.304(2)
$Mo-P_2$	2.325(1)	$P_3\cdots O_2$	3.283(2)
		$P_4\cdots O_1$	3.214(2)
$Mo-P_3$	2.389(1)	$P_4\cdots O_2$	3.183(2)
$Mo-P_4$	2.419(1)		
		$P_1\cdots O_1$	3.289(2)
$Mo-O_1$	2.296(2)	$P_2\cdots O_2$	3.592(2)
$Mo-O_2$	2.337(2)		
		$O_1\cdots O_2$	2.190(3)
$Mo-H$	1.59(4)		
		$P_1\cdots H$	1.94(3)
$P_3\cdots P_1$	3.388(1)	$P_2\cdots H$	2.03(3)
$P_3\cdots P_2$	3.222(1)		
$P_4\cdots P_1$	3.486(1)	$P_3\cdots H$	3.17(3)
$P_4\cdots P_2$	3.506(1)	$P_4\cdots H$	2.73(3)
$P_1\cdots P_2$	3.849(1)		
	Bond Angles (deg)		
P_3MoP_1	92.03(3)	P_1MoH	56(1)
P_3MoP_2	86.22(2)	P_2MoH	59(1)
P_4MoP_1	94.69(3)		
P_4MoP_2	95.27(3)	P_3MoP_4	172.00(9)
P_3MoO_1	89.7(1)	P_1MoP_2	111.88(3)
P_3MoO_2	88.0(1)		
P_4MoO_1	85.9(1)	P_1MoO_1	90.9(1)
P_4MoO_2	84.0(1)	P_2MoO_2	100.8(1)
O_1MoO_2	56.4(1)	P_1MoO_2	147.3(1)
		P_2MoO_1	157.0(1)
P_3MoH	104(1)		
P_4MoH	83(1)	O_1MoH	143(1)
		O_2MoH	155(1)

[a] Figures in parentheses are the estimated standard deviations in the last significant digit. [b] Atoms labeled in agreement with Figure 1 and Tables I and II.

Table IV. Ligand Bond Lengths and Angles Involving Nonhydrogen Atoms in $HMo[P(OCH_3)_3]_4(O_2C_2F_3)$[a]

type[b]	value	type[b]	value
	Distances (Å)		
P_1-O_{11}	1.611(2)	$O_{11}-C_{11}$	1.412(5)
P_1-O_{12}	1.599(2)	$O_{12}-C_{12}$	1.431(5)
P_1-O_{13}	1.597(2)	$O_{13}-C_{13}$	1.446(4)
P_2-O_{21}	1.601(2)	$O_{21}-C_{21}$	1.437(4)
P_2-O_{22}	1.613(2)	$O_{22}-C_{22}$	1.422(4)
P_2-O_{23}	1.607(2)	$O_{23}-C_{23}$	1.419(4)
P_3-O_{31}	1.590(2)	$O_{31}-C_{31}$	1.406(5)
P_3-O_{32}	1.622(2)	$O_{32}-C_{32}$	1.424(5)
P_3-O_{33}	1.621(2)	$O_{33}-C_{33}$	1.436(5)
P_4-O_{41}	1.605(2)	$O_{41}-C_{41}$	1.425(5)
P_4-O_{42}	1.595(3)	$O_{42}-C_{42}$	1.391(6)
P_4-O_{43}	1.598(3)	$O_{43}-C_{43}$	1.328(7)
O_1-C_1	1.240(4)	C_2-F_1	1.294(5)
O_2-C_1	1.243(4)	C_2-F_2	1.258(7)
		C_2-F_3	1.221(5)
C_1-C_2	1.520(4)		
	Bond Angles (deg)		
MoO_1C_1	90.9(2)	$O_{21}P_2O_{22}$	101.8(1)
MoO_2C_2	88.9(2)	$O_{21}P_2O_{23}$	99.3(1)
		$O_{22}P_2O_{23}$	96.0(1)
$O_1C_1C_2$	118.3(3)	$O_{31}P_3O_{32}$	97.4(1)
$O_2C_1C_2$	117.9(3)	$O_{31}P_3O_{33}$	102.6(1)
		$O_{32}P_3O_{33}$	101.0(1)
MoP_1O_{11}	116.1(1)	$O_{41}P_4O_{42}$	102.6(1)
MoP_1O_{12}	125.5(1)	$O_{41}P_4O_{43}$	97.5(1)
MoP_1O_{13}	114.2(1)	$O_{42}P_4O_{43}$	102.5(2)
MoP_2O_{21}	115.0(1)		
MoP_2O_{22}	123.1(1)	$P_1O_{11}C_{11}$	120.3(3)
MoP_2O_{23}	117.4(1)	$P_1O_{12}C_{12}$	122.5(2)
MoP_3O_{31}	119.8(1)	$P_1O_{13}C_{13}$	121.7(3)
MoP_3O_{32}	121.0(1)	$P_2O_{21}C_{21}$	122.8(2)
MoP_3O_{33}	111.9(1)	$P_2O_{22}C_{22}$	121.2(2)
MoP_4O_{41}	119.0(1)	$P_2O_{23}C_{23}$	120.5(2)
MoP_4O_{42}	119.3(1)	$P_3O_{31}C_{31}$	129.2(3)
MoP_4O_{43}	112.8(1)	$P_3O_{32}C_{32}$	119.6(2)
		$P_3O_{33}C_{33}$	121.7(3)
$O_{11}P_1O_{12}$	97.0(1)	$P_4O_{41}C_{41}$	121.3(2)
$O_{11}P_1O_{13}$	97.2(1)	$P_4O_{42}C_{42}$	126.3(4)
$O_{12}P_1O_{13}$	102.1(1)	$P_4O_{43}C_{43}$	130.1(4)

[a] Figures in parentheses are the estimated standard deviations in the last significant digit. [b] Atoms labeled in agreement with Figure 1 and Tables I–III.

$P\cdots H$ and one of the $P\cdots P$ contacts ($P_1\cdots P_2$) are less than the respective van der Waals values by at least 0.30 Å. The extremely short $P_1\cdots H$ and $P_2\cdots H$ contacts appear to indicate an "interaction" between these phosphite ligands and the hydride. Preliminary EHMO calculations[18a] indicate a substantial P-H bond order. It is important to note in this context that the two "girdle" P-Mo-O angles are quite dissimilar and the ~10° opening of the P_2-Mo-O_2 angles are quite dissimilar and the ~10° opening of the P_2-Mo-O_2 angle relative to P_1-Mo-O_1 does not appear to be sterically[18b] induced. Although the two girdle $P\cdots H$ contacts are more than 1.00 Å less than the 3.10-Å van der Waals value, neither of the girdle $P\cdots O$ contacts is less than van der Waals. In fact, the girdle $P_2\cdots O_2$ contact is ~0.30 Å greater than the van der Waals value and is the largest $P\cdots O$ contact on the coordination sphere of **1**. The two equatorial phosphite ligands are oriented in such a way as to produce four $H\cdots O$ van der Waals contacts of 2.52–2.76 Å between the hydride and O_{12}, O_{13}, O_{21}, and O_{22}. These phosphite ligand orientations are shown in Figure 1 and are quite suggestive of five-coordinate phosphorus atoms. H, Mo, P_1, and O_{11} are coplanar to within 0.06 Å while H, Mo, P_2, and O_{23} are coplanar to within 0.08 Å; the H-P_1-O_{11} and H-P_2-O_{23} angles are both 158°.

Short phosphorus-hydrogen nonbonded contacts are well established for transition-metal hydrides with phosphine or phosphite ligands. In the nominally five-coordinate $HM(P\lessdot)_4$ complexes, the MP_4 skeletal array is nearly tetrahedral with no obvious stereochemical impact of the hydride ligand.[18c,19-21] Similar phenomena are documented for the nominally six-coordinate $H_2M(P\lessdot)_4$ complexes where the MP_4 substructure is closer to tetrahedral than to an octahedral fragment.[22] In fact, the phosphorus–hydrogen (metal hydride) separations[22] in *cis*-$H_2Fe[P(C_6H_5)(OC_2H_5)_2]_4$ fall in the range of 2.14–2.30 Å. In both these classes of hydride structures the observed departures from five- and six-coordination polyhedra, respectively, are in the direction expected from purely steric factors. Nevertheless, Hoffmann and co-workers have suggested that the observed coordination geometries may result at least partially from electronic factors.[23] In $HMo[P(OCH_3)_3]_4[O_2CCF_3]$ the distortion is in a direction that is counter to steric predictions. For example, we might treat **1** as a pseudo-five-coordinate complex by ignoring the hydride ligand and by treating the trifluoroacetate group as a unidentate ligand. As a result of this structural decomposition, the coordination geometry becomes a trigonal bipyramid with axial phosphite ligands. Interestingly, the P-Mo-P angle in the equatorial plane is not greater than 120° to allow for the presence of the stereochemically pseudo or phantom hydride ligand, but less than 120°—specifically 111.9°. The observed reduction in this angle is suggestive of a real electronic effect as suggested by Hoffmann and his co-workers.

The relative axial and equatorial Mo-P bond lengths, listed in Table III, are unusual for pentagonal bipyramidal geometry. The minimization of nonbonding repulsions between pairs of contiguous coordinated atoms in the tightly packed pentagonal

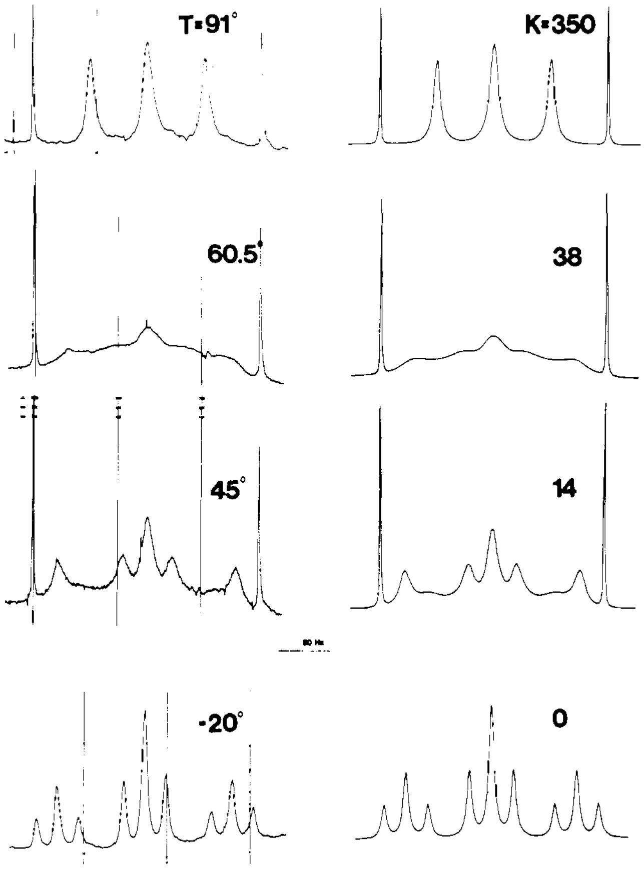

Figure 2. Variable-temperature ^1H NMR of $HMo[P(OCH_3)_3]_4[O_2CCF_3]$ in toluene-d_8 and spectra calculated on the basis of nonpairwise exchange.

girdle of a D_{5h} ML_7 species generally produces two sets of M–L bonds with the equatorial set longer than the axial set.[24] In the specific case of d^4-pentagonal bipyramidal complexes, theoretical analyses place the axial bonds essentially equivalent in strength[25] to or slightly greater[4] than those of the equatorial bonds. For example, the d^4 pentagonal bipyramidal $Mo(CN)_7{}^{2-}$ has all Mo–C bonds essentially equivalent in length[26] and in a related d^4 hydride complex, $H_4Os[P(C_6H_5)(CH_3)_2]_3$, the axial Os–P distances are 0.03–0.04 Å shorter than the one equatorial Os–P bond.[27] In **1** the axial Mo–P bonds average 2.404 (1, 14, 15, 2) Å[28] while the equatorial bonds average 2.323 (1, 2, 2, 2) Å.[28] This relatively large difference which is counter to established[3,4] bond distance ratios in d^0–d^4 pentagonal bipyramidal structures and also to theoretical predictions is significant and is not easily rationalized. In treating this complex as a pseudo-five-coordinate structure, however, the relative axial and equatorial Mo–P bond lengths do conform to theory and to experimental results (*for a trigonal bipyramidal structure*). The short equatorial Mo–P distances contribute to the aforementioned short P···H contacts. These two apparent structural anomalies are unquestionably interrelated and probably have their origins in electronic effects.[23] It is of interest to note that in *cis*-$H_2Fe[P(C_6H_5)(OC_2H_5)_2]_4$ the two phosphorus atoms which are cis to (and *very* close to) the hydride ligands have shorter (0.02–0.03 Å) bonds to the iron atom than the other two and ~trans phosphorus atoms[22]—an effect that is also counter to steric considerations.

The remainder of the bond lengths and angles involving nonhydrogen atoms of **1** are rather unexceptional. The Mo–H bond length of 1.59 (4) Å in **1** is a reasonable X-ray value compared with the average X-ray value of 1.70 (11, 5, 9, 4) Å observed for the Mo–H bonds in a formally eight-coordinate tetrahydridomolybdenum(IV) species[29] and the value of 1.685 (3) Å for Mo–H determined from a neutron diffraction study of $(\eta^5\text{-}C_5H_5)_2MoH_2$.[30] Trifluoroacetate bond distances are normal for a nonbridging bidentate acetate ligand compared with those for related ligands in other systems.[31] The four-atom $-Mo\text{-}O_1\text{-}C_1\text{-}O_2-$ chelate ring is folded by only 2.7° along the $O_1 \cdots O_2$ polyhedral edge; Mo, O_1, O_2, C_1, and C_2 are coplanar to within 0.03 Å. The following average parameters for the trimethyl phosphite ligands are also normal compared with those determined[1,32] for this ligand in other complexes: P–O, 1.605 (2, 8, 17, 12) Å;[28] O–C, 1.415 (5, 20, 87, 12) Å; O–P–O, 99.8 (1, 24, 38, 12)°; P–O–C, 123.1 (3, 27, 70, 12)°. The 0.93 (6, 6, 25, 36) Å average C–H bond length for the trimethyl phosphite ligands in **1** is a normal X-ray value for this bond and is in excellent agreement with those determined by high-precision X-ray studies [33] of other compounds; the average value of 109 (4, 8, 30, 72)° for the O–C–H and H–C–H angles is essentially the idealized tetrahedral value. Exclusive of the short ligand–ligand contacts discussed above, there are no intra- or intermolecular contacts which are significantly less than the van der Waals[17] value.

Table VI. Permutation Analysis of $HMo[P(OCH_3)_3]_4[O_2CCF_3]$ under C_{2v} Constraint

equivalent basic permutational set	permutations[a]	
identity and inverse	(12) (34)	(12) (34)
pairwise exchange	(13) (24)	(1423)
	(1324)	(14) (23)
nonpairwise exchange	(23)	(243)
	(234)	(24)
	(132)	(1432)
	(1342)	(142)
	(123)	(1243)
	(13)	(143)
	(1234)	(124)
	(134)	(14)

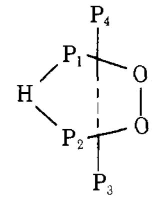

[a] Relative to structure shown.

Dynamic Stereochemistry of $HMo[P(OCH_3)_3]_4[O_2CCF_3]$. The X-ray crystallographic structure of $HMo[P(OCH_3)_3]_4[O_2CCF_3]$ predicts a ground-state AB_2CX spin system where A and C represent the nonequivalent axial phosphorus sites generated by the minor displacement of the hydride ligand out of the equatorial plane of an idealized pentagonal bipyramid. Between −100 and 20 °C, however, the hydride resonance is observed as a triplet of triplets, the X part of an A_2B_2X spin system. This spectrum is the expected one as the barrier for Mo–H bending in the plane of the molybdenum and the axial phosphorus atoms should be exceedingly small. Indeed, the observed A_2B_2X pattern is consistent with any low-energy fluxional process involving the hydride ligand.

Above −20 °C, the hydride resonances for the molybdenum complex coalesce to give ultimately (95 °C) a spectrum approaching a binomial quintet. Retention of two sharp transitions in the intermediate exchange region establishes the intramolecular nature of the phosphorus exchange. Permutational analysis[34] under a C_{2v} structural constraint factors the 4! phosphorus permutations into two NMR-differentiable sets (Table VI), which by analogy to previously studied systems[35,36] can be labeled pairwise and nonpairwise exchange. Nonpairwise exchange represents the exchange of a single axial–equatorial pair while pairwise exchange represents the simultaneous exchange of both axial sites with both equatorial sites. The line shapes calculated for intermediate exchange rates based on pairwise and nonpairwise exchange permutations differ appreciably. The major difference is in the central transition, which collapses for nonpairwise processes and is unperturbed for pairwise exchange. In both cases, the outermost transitions are unperturbed by exchange.

In the intermediate exchange region, the experimental spectra closely resemble spectra calculated on the basis of nonpairwise exchange (Figure 2).[37] An Eyring plot of the resultant temperature–rate correlation is linear with a correlation coefficient of 0.997 giving $\Delta H^{\ddagger} = 15.7 \pm 0.4$ kcal/mol and $\Delta S^{\ddagger} = -4 \pm 1$ eu.

Simple idealized pathways have been proposed for the interconversion of pentagonal bipyramidal, capped octahedral, and capped trigonal prismatic geometries.[15,39] A pentagonal bipyramid to capped trigonal prism interconversion, which has been observed for $TaCl(\eta^4\text{-}C_{10}H_8)(dmpe)_2$,[40] was anticipated to be a low-barrier process for the molybdenum complex, but this rearrangement permutationally constitutes a pairwise exchange of the phosphorus atoms. Only by multiple applications of rearrangements by idealized geometric pathways can nonpairwise mechanisms be generated.

Mechanisms not based on the idealized pathways can account for nonpairwise exchange. Rotation by 120° of a triangular face formed by three phosphites is one such possibility. The presence of an intermediate of finite concentration in a pairwise exchange process could also account for the observed spectra. Thus, the data rule out pairwise *mutual* exchange processes but do not distinguish among the remaining possibilities. In previously studied seven-coordinate monohydride complexes[35,36] both pairwise and nonpairwise exchange have been observed. Pairwise exchange has been rationalized by mechanisms involving hydride migration. Nonpairwise exchange in these hydride complexes, as in our molybdenum hydride, cannot be explained by hydride migration or by the simple geometric pathways that interconnect idealized seven-coordinate geometries. A satisfactory structural and theoretical understanding of these dynamic phenomena does not exist presently.

Acknowledgments. We thank the University of Nebraska Computing Center for a generous grant of computer time, the National Science Foundation, and the donors of the Petroleum Research Fund, administered by the American Chemical Society, for support of the noncrystallographic studies.

Supplementary Material Available: A listing of anisotropic thermal parameters for nonhydrogen atoms (Table II), bond lengths and angles involving hydrogen atoms of the trimethyl phosphite ligands (Table V), and observed and calculated structure factors from the final cycles of least-squares refinement (34 pages). Ordering information is given on any current masthead page.

References and Notes

(1) For synthetic and chemical background and a preliminary account of structure and stereochemistry, cf. Muetterties, E. L.; Kirner, J. F.; Evans, W. J.; Watson, P. L.; Abdel-Meguid, S.; Tavanaiepour, I.; Day, V. W. *Proc. Natl. Acad. Sci. U.S.A.* **1978**, *75*, 1056.

(2) (a) Department of Chemistry, University of Toronto, Toronto, Ontario, Canada M5S 1A1. (b) University of California. (c) University of Nebraska. (d) Camille and Henry Dreyfus Teacher–Scholar.

(3) Drew, M. *Prog. Inorg. Chem.* **1977**, *23*, 67.

(4) Hoffmann, R.; Beier, B. F.; Muetterties, E. L.; Rossi, A. R. *Inorg. Chem.* **1977**, *16*, 511.

(5) "International Tables for X-ray Crystallography", Vol. I, "Symmetry Groups"; Kynoch Press: Birmingham, England, 1969; p 99.

(6) "International Tables for X-ray Crystallography", Vol. III, "Physical and Chemical Tables"; Kynoch Press: Birmingham, England, 1968; p 166.

(7) Cromer, D. T.; Mann, J. L. *Acta Crystallogr., Sect. A* **1968**, *24*, 321.

(8) Cromer, D. T. *Acta Crystallogr.* **1965**, *18*, 17.

(9) Zachariasen, W. H. *Acta Crystallogr.* **1967**, *23*, 558.

(10) See paragraph at end of paper regarding supplementary material.

(11) Kleier, D. A.; Binsch, G. Quantum Chemistry Program Exchange No. 165.

(12) Bushweller, C. H.; Bhat, G.; Letendre, L. J.; Brunelle, J. A.; Bilofsky, H. S.; Ruben, H.; Templeton, D. H.; Zalkin, A. *J. Am. Chem. Soc.* **1975**, *97*, 65.

(13) The plane described by the equation $0.115X + 0.989Y + 0.087Z = 3.394$ where X, Y, and Z are orthogonal coordinates along $\vec{\mathbf{a}}$, $\mathbf{b}$, and $\vec{\mathbf{c}}^*$, respectively, of the crystal system.

(14) Mean plane defined by $0.733X - 0.169Y + 0.659Z = 1.703$ with each atom coplanar to within 0.13 Å.

(15) Muetterties, E. L.; Guggenberger, L. J. *J. Am. Chem. Soc.* **1974**, *96*, 1748.

(16) Cf. discussion of the application of the dihedral angle criterion to coordination polyhedra with diverse ligand atoms by Kouba, J. K.; Wreford, S. S. *Inorg. Chem.* **1976**, *15*, 1463, and also ref 3.

(17) Pauling, L. "The Nature of the Chemical Bond", 3rd ed.; Cornell University Press: Ithaca, N.Y., 1960; p 260.

(18) (a) EHMO calculations using QCPE No. 256 and coordinates derived from the crystallographic study indicate substantial bonding interaction between the hydride and both P_1 and P_2. Mulliken bond orders are Mo–H, 0.2767; P_1–H, 0.2649; P_2–H, 0.2630. Moving the hydride ligand up or down 26° (from the position in the crystallographic structure) in the MoP_3P_4 plane did not significantly change the total energy (~0.15 eV). In raising the hydride, the P_1–H and P_2–H bond orders decreased, which was compensated by an increase in the P_4–H bond order. (b) In the EHMO calculations,[18a] the trifluoroacetate ligand was shifted to a symmetrical site trans to Mo–H. The calculational results for this geometry were not significantly different from those based on the crystallographic structure. Bond orders, formal charges, and total energies were essentially identical for the two calculations. (c) Meakin, P.; Muetterties, E. L.; Jesson, J. P. *J. Am. Chem. Soc.* **1972**, *94*, 5271.

(19) Baker, R. W.; Pauling, P. *Chem. Commun.* **1969**, 1495.

(20) Baker, R. W.; Maier, B. V. L.; Pauling, P.; Nyholm, R. S. *Chem. Commun.* **1970**, 1077.

(21) Titus, D. D.; Orio, A. A.; Marsh, R. E.; Gray, H. B. *Chem. Commun.* **1971**, 322.

(22) Guggenberger, L. J.; Titus, D. D.; Flood, M. T.; Marsh, R. E.; Orio, A. A.; Gray, H. B. *J. Am. Chem. Soc.* **1972**, *94*, 1135.

(23) (a) Hoffmann, R.; Howell, J. M.; Rossi, A. R. *J. Am. Chem. Soc.* **1976**, *98*, 2484. (b) Elian, M.; Hoffman, R. *Inorg. Chem.* **1975**, *14*, 1058.

(24) (a) Park, J. J.; Collins, D. M.; Hoard, J. L. *J. Am. Chem. Soc.* **1970**, *92*, 3636. (b) von Dreele, R. B.; Stezowski, J. J.; Fay, R. C. *Ibid.* **1971**, *93*, 2887.

(25) Shustorovich, E. *Inorg. Chem.* **1978**, *17*, 2648.

(26) Drew, M. G. B.; Mitchell, P. C. H.; Pygall, C. F. *J. Chem. Soc., Dalton Trans.* **1977**, 1071.

(27) Hart, D. W.; Bau, R.; Koetzle, T. F. *J. Am. Chem. Soc.* **1977**, *99*, 7557.

(28) The first number in parentheses following an averaged value for a bond length or angle is the root-mean-square estimated standard deviation of an individual datum. The second and third numbers, when given, are the average and maximum deviations from the average value, respectively; the fourth number is the number of individual values included in the average.

(29) Guggenberger, L. J. *Inorg. Chem.* **1973**, *12*, 2295.

(30) Schultz, A. J.; Stearley, K. L.; Williams, J. M.; Mink, R.; Stucky, G. D. *Inorg. Chem.* **1977**, *16*, 3303.

(31) (a) Mealli, C.; Midollini, S.; Sacconi, L. *Inorg. Chem.* **1975**, *14*, 2513. (b) LaMonica, G.; Cenini, S.; Forni, E.; Manessero, M.; Albano, V. G. *J. Organomet. Chem.* **1976**, *112*, 297. (c) Drew, M. G. B.; Otham, A. H. N. C.; Edwards, D. A.; Richards, R. *Acta Crystallogr., Sect. B* **1975**, *31*, 2695. (d) Grdenic, D.; Kamenar, B.; Hergold-Brundic, A. *Cryst. Struct. Commun.* **1976**, *5*, 769.

(32) Goh, L.-Y.; D'Aniello, Jr., M. J.; Slater, S.; Muetterties, E. L.; Tavanaiepour, I.; Chang, M. I.; Fredrich, M. F.; Day, V. W. *Inorg. Chem.* **1979**, *18*, 192.

(33) (a) Cotton, F. A.; Day, V. W.; Hazen, Jr., E. E.; Larsen, S. *J. Am. Chem. Soc.* **1973**, *95*, 4834. (b) Cotton, F. A.; Day, V. W.; Hazen, Jr., E. E.; Larsen, S.; Wong, S. T. K. *Ibid.* **1974**, *96*, 4471. (c) Baumgarten, H. E.; McMahan, D. G.; Elia, V. J.; Gold, B. I.; Day, V. W.; Day, R. O. *J. Org. Chem.* **1976**, *41*, 3798. (d) Churchill, M. R. *Inorg. Chem.* **1973**, *12*, 1213.

(34) Jesson, J. P.; Meakin, P. *Acc. Chem. Res.* **1973**, *6*, 269.

(35) Meakin, P.; Guggenberger, L. J.; Tebbe, F. N.; Jesson, J. P. *Inorg. Chem.* **1974**, *13*, 1025.

(36) Datta, S.; Dezube, B.; Kouba, J. K.; Wreford, S. S. *J. Am. Chem. Soc.* **1978**, *100*, 4404.

(37) Careful study of the hydride spectra revealed a small temperature dependence to the phosphorus hydride coupling constants. In the temperature range −30 to 10 °C the two phosphorus hydride coupling constants each increased 0.025 Hz/deg. In the temperature range −30 to 91 °C $J_{P_AH} + J_{P_BH}$ increased 0.05 Hz/deg. Temperature dependence of coupling constants can result from temperature-dependent equilibria or from population of vibrational modes which change the position of the coupled nuclei.[38] A study of the effect of temperature on the coupling constants and chemical shifts in this molecule revealed no behavior which can be unambiguously assigned to the presence of two or more equilibrating species.

(38) (a) Gutowsky, H. S.; Mochel, V. D.; Somers, B. G. *J. Chem. Phys.* **1962**, *36*, 1119. (b) Ramey, K. D.; Brey, W. S. *J. Chem. Phys.* **1966**, *40*, 2349.

(39) Brown, L. D.; Datta, S.; Kouba, J. K.; Smith, L. K.; Wreford, S. S. *Inorg. Chem.* **1978**, *17*, 729.

(40) Albright, J. O.; Datta, S.; Dezube, B.; Kouba, J. K.; Marynick, D. S.; Wreford, S. S.; Foxman, Bruce M. *J. Am. Chem. Soc.* **1979**, *101*, 611.